Experimental study of the hydrodynamic interaction between a fish and an actively pitching airfoil

Rishita Das^{a,b}, Sean D. Peterson^c, and Maurizio Porfiri^{a,b}

^aDepartment of Mechanical and Aerospace Engineering, Tandon School of Engineering, New York University, Brooklyn, New York, 11201, USA

^bCenter for Urban Science and Progress, New York University, Brooklyn, New York, 11201, USA

^cDepartment of Mechanical and Mechatronics Engineering, University of Waterloo, Waterloo, Ontario N2L 3G1, Canada

ABSTRACT

The phenomenon of fish schooling - coordinated swimming of fish in polarized groups of specific spatial formations - is commonly observed in several species of fish. Fish schooling may even provide hydrodynamic advantages reducing the overall swimming cost of the group. To date, the role of hydrodynamics in coordinated swimming is not completely understood as it is difficult to separately study the role of hydrodynamic interaction from other forms of interaction between the fish. Here, we propose a statistical methodology based on information theoretic tools and flow velocity measurements, that can potentially tease out the hydrodynamic interaction pathways from visual and tactile ones. To avoid experimental confounds from bidirectional interactions and objectively understand cause-and-effect relationships, we design a robotic platform that mimics the behavior of two fish swimming in-line in a controlled setup inside a water channel. We examine the response of a flag to the fish-like unsteady wake generated by an actively pitching airfoil located upstream. We systematically quantify the passive hydrodynamic effect by studying the flapping motion of the flag located downstream of the airfoil in response to both periodic pitching and less predictable, random startling motion of the upstream airfoil. The study integrates experimental biomimetics with information theory to establish a deeper understanding of hydrodynamics in fish schooling.

Keywords: Fluid dynamics, Fish schooling, Information theory, Unsteady hydrodynamics

1. INTRODUCTION

Most species of fish live and swim together in groups, which provides them advantages in terms of escaping predators, searching for food, mating, and finding optimal routes. ^{1–4} Living in groups, they often swim close to each other in crystallized spatial formations, ^{5,6} such as side-by-side (phalanx), in-line, and staggered (diamond) configurations, ^{7–9} which likely reduces the overall swimming cost of the collective. ^{7,10,11} Fish interact through different sensory cues including hydrodynamic, visual, vestibular, and tactile. The collective behavior observed in fish is a complex integration of all these physical pathways, making it difficult to understand the role of each of them. In this work, we propose an information-theoretic approach to experimentally disentangle these pathways, specifically segregating hydrodynamic interactions from the remaining pathways. For this, we rely on the concept of transfer entropy. ^{12,13} as a measure of causal interaction between two individually functional entities. Transfer entropy, which is universally employed to study causality in complex systems, has seen relatively limited use in the field of fluid dynamics and fluid-structure interaction.

To avoid the confounding effects of bidirectional interactions, presence of non-hydrodynamic pathways, and intermittent interactions in experiments with live fish, we establish the performance of our method on a fluid-structure interaction problem resembling a subsystem of a fish school. We design an experimental setup in a water

Further author information: (Send correspondence to Maurizio Porfiri)

Rishita Das: E-mail: rd3154@nyu.edu

Sean D. Peterson: E-mail: peterson@uwaterloo.ca

Maurizio Porfiri: E-mail: mporfiri@nyu.edu, Telephone: +1 646 997 3681

channel with a robotic pitching mechanism that produces a fish-like wake and a compliant object downstream that readily responds to the generated unsteady vortices, similar to a downstream swimming fish. The setup consists of an actively controlled airfoil which is positioned upstream and a focal subject (flag) that is flapping downstream, in the unsteady wake of the pitching airfoil. To study schooling of fish pairs, researchers have commonly investigated the response of an airfoil in the wake of another pitching airfoil in a channel flow.^{14–16} While such a setup provides an approximate sense of the passive hydrodynamic response of a fish swimming downstream of another fish, it does not exactly replicate the undulating response of a fish body, and can only capture close-range interaction. Thus, in this work we study the motion of a flag, which can undergo body undulations and sustain longer-range interaction with the upstream airfoil, providing a closer approximation to the response of a fish.

2. EXPERIMENTAL SETUP

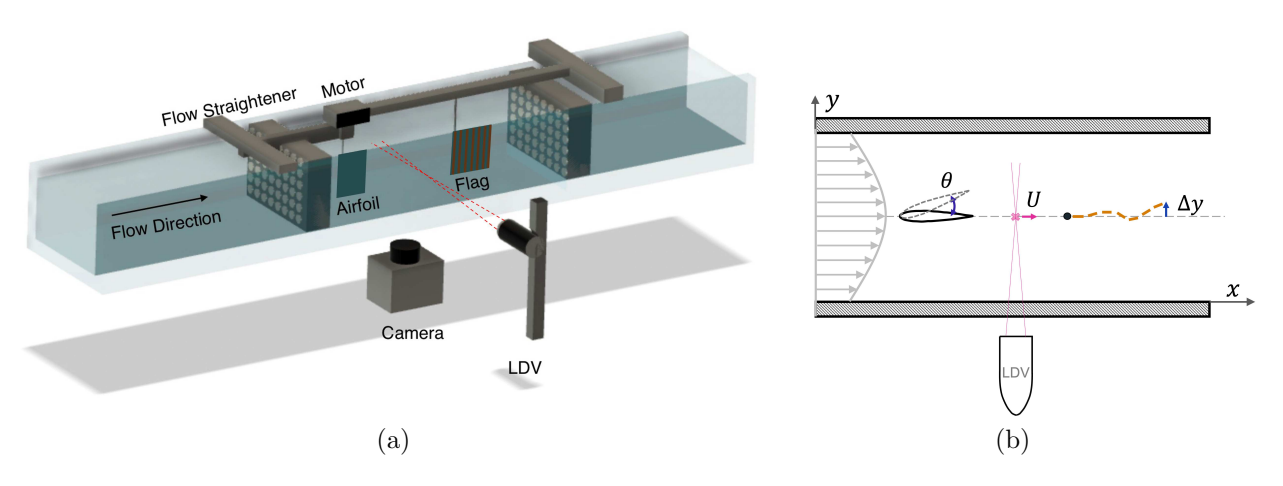


Figure 1. Experimental setup in a water channel: (a) 3D view of the test section with an upstream airfoil and a downstream flag, a camera recording the bottom view of the test section, and laser Doppler velocimetry system measuring the streamwise flow velocity between the airfoil and the flag; (b) 2D view of the test section as captured by the camera.

Experiments are conducted in a 29 cm \times 10 cm \times 15 cm test section inside an open water channel (Engineering Laboratory Design, Inc.) as shown in Fig. 1(a). Two honeycomb flow straighteners are placed on either side of the test section to ensure straight and undisturbed inflow into the test section. A 3D printed NACA 0012 airfoil of chord length c=5 cm and span 6.9 cm is placed upstream in the test section, and allowed to undergo pitching motion about a pivot shaft at 20% of the airfoil chord length. The airfoil is fixed in position while its pitching motion is actively controlled by a servo-motor using an Arduino Uno microcontroller board and programmed via Arduino 1.8.19 software package. A periodic pitching motion of frequency 3 Hz and amplitude 12° is interspersed with a random startling motion of 40° in a randomly selected direction with a randomly generated time interval between startles (uniformly distributed in 5 ± 1.5 s).

A 6.98 cm \times 6.9 cm ribbed flag is designed using a 1 mm-diameter flag pole, a continuous Mylar sheet covering the entire area of the flag, twelve 4 mm \times 69 mm copper strips pasted on either side of the Mylar sheet forming ribs of the flag, and two 7 mm \times 69 mm copper strips pasted on either side of the Mylar sheet but also rigidly fixed to the pole. The design of the flag, specifically its bending stiffness and mass density, ensures its flexibility and ability to flap, 17,18 its instability toward flutter in high enough flow speeds (\geq 0.5 m/s), and the absence of any torsional motion about the streamwise or spanwise axes. The flag is fixed in position at a distance of 5.4 cm downstream from the airfoil and allowed to passively flap in response to the unsteady flow structures generated by the pitching airfoil in its upstream.

The two-dimensional view of the test section from the bottom of the water tunnel (Fig. 1b) including the motion of the airfoil and the flag is captured by a high-speed camera that records at 60 frames/s. A free and open source software, OBS Studio, is used to record the videos at a resolution of 1920×1080 pixels of a test section

view of 29 cm \times 15 cm. The pitching angle of the airfoil, $\theta(t)$, and the spanwise deflection of the tip of the flag, $\Delta y(t)$, are tracked by a program developed in MATLAB R2021b using utilities available in its image processing toolbox. A Dantec Dynamics laser Doppler velocimetry (LDV) system is used to measure the instantaneous streamwise component of flow velocity, U(t), at a point in the channel centerline between the airfoil and the flag (3 cm downstream of the airfoil trailing edge). The LDV measurement of U(t) is recorded for the complete duration of each experiment using the BSA Flow software. Since LDV relies on the light scattering caused by particles in the flow, the measurement of U(t) is non-uniformly spaced in time. In each experiment, the video of the test section view and the LDV measurement of flow velocity are recorded for a duration of 180 s. The inflow speed in the test section is maintained at $U_0 = 0.39$ m/s at the centerline (recorded using LDV), that is, with a water channel frequency of 19 Hz. This represents a flow Reynolds number of $Re = U_0 c/\nu = 21850$ based on the airfoil chord length.

3. STATISTICAL METHOD

In information theory, the uncertainty of a random variable, X, is encoded by Shannon entropy, ¹⁹

$$H(X) = -\sum_{x \in \chi} p(x) \log p(x), \tag{1}$$

where p(x) is the probability of occurrence of the realization x in the set of all possible realizations χ , and $-\log p(x)$ is the surprisal or information content of x.¹³ The joint entropy of two random variables, X and Y, and the conditional entropy of X given Y are given by

$$H(X,Y) = -\sum_{x \in \chi, y \in \gamma} p(x,y) \log p(x,y) \quad \text{and} \quad H(X|Y) = -\sum_{x \in \chi, y \in \gamma} p(x,y) \log p(x|y), \tag{2}$$

respectively. Extending these concepts to two discrete-time stationary random processes, $X = \{X_n\}_{n=1,2,...}$ and $Y = \{Y_n\}_{n=1,2,...}$, where n is the time index, one can detect causal influence²⁰ of X on Y by applying transfer entropy^{12,21} defined as

$$TE_{X\to Y} = H(Y_n|Y_{n-1}) - H(Y_n|Y_{n-1}, X_{n-\delta})$$

$$= \sum_{y_n, y_{n-1}, x_{n-\delta}} p(y_n, y_{n-1}, x_{n-\delta}) \log \left[\frac{p(y_n|y_{n-1}, x_{n-\delta})}{p(y_n|y_{n-1})} \right].$$
(3)

Transfer entropy from X to Y measures the reduction in uncertainty in the current state of the target (Y_n) from its past state (Y_{n-1}) , due to the knowledge about the state of the source δ time-steps in the past $(X_{n-\delta})$. Here, we consider the dependence of the target's behavior on only a single time-history of the source and itself. Similarly, $TE_{Y\to X}$ measures the causal influence of Y on X. In the case of asymmetric causal influence between X and Y, net transfer entropy, net $TE_{X\to Y} = TE_{X\to Y} - TE_{Y\to X}$ reflects the net direction of causal interaction.

In the presence of another random process Z, related with X and/or Y, one can compute conditional transfer entropy²²

$$TE_{X\to Y|Z} = H(Y_n|Y_{n-1}, Z_{n-\delta_2}) - H(Y_n|Y_{n-1}, X_{n-\delta}, Z_{n-\delta_2})$$

$$= \sum_{y_n, y_{n-1}, x_{n-\delta}, z_{n-\delta_2}} p(y_n, y_{n-1}, x_{n-\delta}, z_{n-\delta_2}) \log \left[\frac{p(y_n|y_{n-1}, x_{n-\delta}, z_{n-\delta_2})}{p(y_n|y_{n-1}, z_{n-\delta_2})} \right]. \tag{4}$$

that represents the statistical causal dependence of Y on the δ -delayed past state of X, accounting for the knowledge of its own past and the past of Z at a delay of δ_2 time-steps.

In this study, we utilize these information-theoretic measures to infer the cause-and-effect relationship between the upstream airfoil and the downstream flag, and specifically isolate the flow-mediated interaction pathway. One of the difficulties in computing transfer entropy is the accurate estimation of the high-dimensional probability density function, which restricts the binning of the sample space in each dimension. To avoid this issue, we use the dynamics-based symbolic approach²³ with an embedding dimension of m = 2, which symbolizes each time-series into only two bins per dimension resulting in highly accurate statistical estimation, and is also more robust to noise in the time-series.

4. DATA ANALYSIS

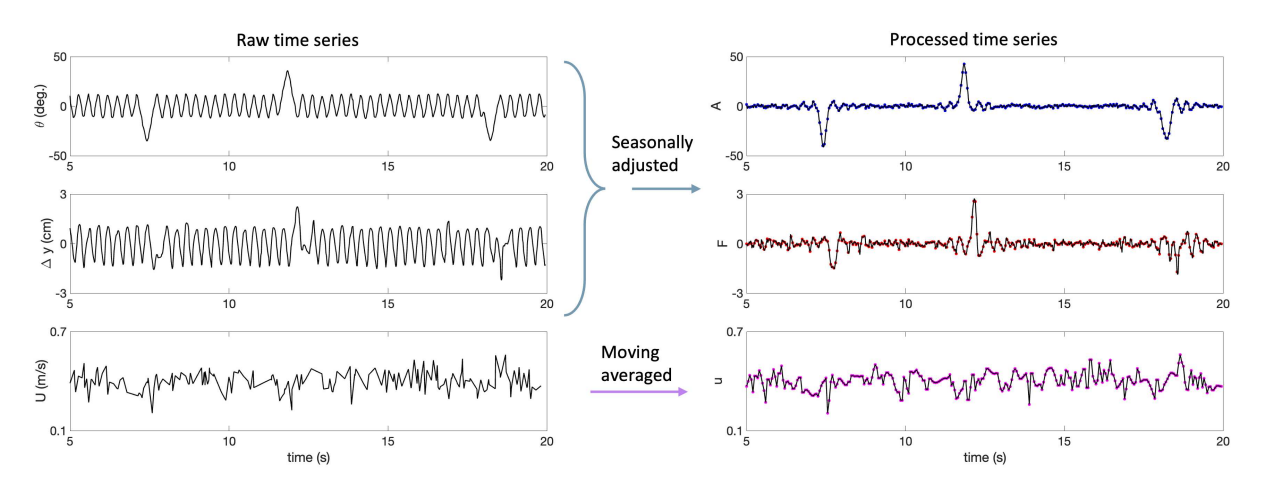


Figure 2. Sample portion of raw time-series (left) and processed time-series (right) of the airfoil pitching angle, flag tip deflection, and streamwise flow speed recorded by LDV. The colored dots in the plots on the right represent the downsampled time-series of data used for symbolization and in transfer entropy analysis.

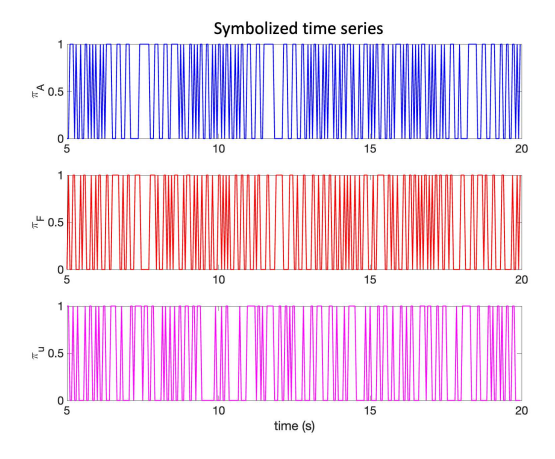


Figure 3. Sample portion of symbolized time-series of the airfoil pitching angle, flag tip deflection, and streamwise flow speed recorded by LDV used for the transfer entropy analysis.

From the conducted experiments, the raw time-series of the airfoil pitching angle θ and flag tip deflection Δy are recorded at a uniformly spaced frequency of 60 Hz, as shown in the left column of Fig. 2. As actuated by the motor, the pitching of the airfoil consists of periodic oscillations of θ , intermixed with startling motions occurring at random time intervals. It is evident that the flag flaps in response to the airfoil pitching and the unsteady flow vortices generated by it. In fact, the deflection of the flag also shows the periodic oscillations along with abrupt changes in behavior following the startles of the airfoil. There is a clear delay (~ 0.35 s) in the flag's response with respect to the airfoil motion, as the interaction is mediated by the flow and, therefore, this delay is likely an inverse function of the speed of the channel flow. Note that the periodic pitching causes a continuous interaction between the airfoil and the flag through the flow, while the random startle behavior ensures that the measured time-series of airfoil and flag motions are stochastic in nature, resulting in effective application of statistical methods for causal inferences. Unlike the time-series of the airfoil and the flag, the instantaneous streamwise flow speed U is non-uniformly spaced with an average of approximately 15 data points per second. Due to the high Reynolds number, the recorded instantaneous flow speed is relatively more noisy without any

noticeable impact of the periodic oscillations or startling behavior of the airfoil on it.

Before performing the information-theoretic analysis, preprocessing of the data is important to align all the time-series and mitigate the effects of any measurement noise. First, we seasonally adjust the θ and Δy time-series, by using the Multiple Seasonal-Trend decomposition using LOESS (MSTL) package in Python 3.9.7 to remove the "seasonal" trends in the data, yielding the processed time-series of A for the airfoil's and F for the flag's movements, as shown in the right column of Fig. 2. These time-series clearly encapsulate the startling behavior, discarding the majority of the periodic oscillations (seasonality). Then, to eliminate any experimental noise associated with mechanical motions or measurements, the time-series are downsampled to 20 data points per second from the recorded 60 frames per second. Finally, for the non-uniformly spaced data of U recorded by LDV, we first obtain the moving average of the data over 0.05 s windows to generate a uniformly-spaced average measure, u, that matches in time with the downsampled time-series of A and F. These time-series are then symbolized with embedding dimension m = 2 (as per section 3) to obtain π_A , π_F , and π_u (Fig. 3), which attain binary values 0 and 1 depending on whether there is a decrease or an increase in the value of the time-series from a given time step to the next one. These symbolized time-series are finally used in computing the information-theoretic measures.

5. RESULTS

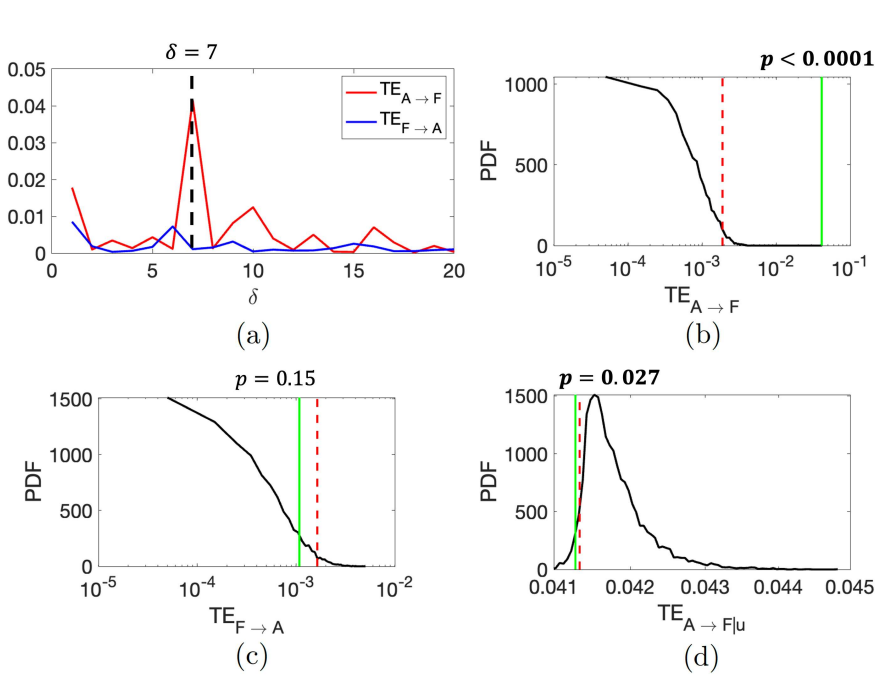


Figure 4. (a) Transfer entropy from airfoil (A) to flag (F) and from flag to airfoil for different delays δ (in time-steps) of F with respect to A. At the peak delay of $\delta = 7$, the (b) transfer entropy from airfoil to flag and its surrogate distribution, (c) transfer entropy from flag to airfoil and its surrogate distribution, and (d) conditional transfer entropy from airfoil to flag, conditioned on the instantaneous flow speed u. Green solid lines represent the values of transfer entropy (or conditional transfer entropy), and red dashed lines mark the 95 (or 5) percentile cutoff of their surrogate distributions.

The transfer entropy from the airfoil to the flag and vice versa are computed using Eq. (3) and plotted as a function of the delay between the flag and the airfoil in Fig. 4(a). It is evident that $TE_{A\to F}$ is generally greater than $TE_{F\to A}$ at most delays, implying a positive net $TE_{A\to F}$. The peak $TE_{A\to F}$ is achieved at a delay of $\delta=7$ time-steps = 0.35 s as expected from the time-series in Fig. 2. The remaining analysis is done at this peak delay between the flag and the airfoil. The surrogate distributions are generated for transfer entropy in each of the two directions by randomly shuffling the symbolized time-series of the source 10,000 times, while maintaining the self dynamics of the target (for $TE_{A\to F}$, we shuffle A). Figs. 4(b,c) illustrate the probability density function of these

shuffled surrogate time-series to test the significance of the transfer entropy values we obtained from the true time-series of the experiments. Clearly, $\text{TE}_{A\to F}$ is significantly higher than chance (p<0.0001), suggesting that there exists a causal interaction from the actively actuated upstream airfoil to the passively flapping downstream flag. On the other hand, $\text{TE}_{F\to A}$ is not indistinguishable from chance (p=0.15), indicating that the direction of the flow is important as the flow mediates the interaction between the airfoil and the flag. As a result, no significant causal influence is observed from the flag downstream on the airfoil upstream.

Next, we further condition the transfer entropy from the airfoil to the flag, on the flow information encoded in the time-series of instantaneous flow speed (u) at a point between the airfoil and the flag, using Eq. (4). The delay between the flag and the flow speed is chosen $(\delta_2 = 4)$ so as to minimize the conditional transfer entropy. The obtained conditional transfer entropy $\text{TE}_{A \to F|u}$ is smaller than $\text{TE}_{A \to F}$ in value. To determine the significance of this conditioning on u and test its implication on the measure of causal interaction between the source (A) and the target (F), we obtain a surrogate distribution of the conditional transfer entropy breaking the link with conditional variable (u). The surrogate distribution is obtained by shuffling the time-series of u, while keeping the dynamics between F and F interaction in Fig. 4(d), the value of F is found to be significantly reduced (p = 0.027), demonstrating that conditioning on the flow information collected by the LDV reduces the causal interaction significantly more than conditioning on any random time-series with irrelevant information.

6. CONCLUSIONS

In this work, we present a controllable robotic mechanism to investigate fish schooling and study fluid dynamic interactions between fish as they swim in-line. The system consists of an actively pitching airfoil in a flow, generating unsteady flow structures similar to that of a leading fish, and continuously interacting with a passively flapping flag situated downstream, alike a following fish. Preliminary experimental findings demonstrate that the flag responds to both the periodic as well as startling motions of the pitching airfoil, resembling the behavior of a fish swimming in the wake of a leading fish.

We demonstrate that the information-theoretic measure of transfer entropy successfully quantifies the causal influence of the motion of the airfoil on the deflection of the flag. Further, conditioning transfer entropy on the streamwise flow speed at a point between the airfoil and the flag significantly reduces the causal hydrodynamic influence of the airfoil on the flag. This suggests that with the knowledge of the state of the flow, it may be possible to quantify the hydrodynamic influence of the source on the target in the flow. The proposed diagnostic methodology reduces the causal influence to effectively zero since fluid dynamics is the only pathway of interaction; in more complex scenarios, where other influences are important, this method can be extended to segregate one interaction pathway from another. One of the overarching ideas is that such a tool will help disentangle the different sensory mechanisms underlying fish schooling.

ACKNOWLEDGMENTS

The research was supported by the National Science Foundation under Grant No. CMMI-1901697. The authors would also like to thank Ms. Aishwarya Ravindran for her help during experiments.

REFERENCES

- [1] Major, P. F., "Predator-prey interactions in two schooling fishes, caranx ignobilis and stolephorus purpureus," *Animal Behaviour* **26**, 760–777 (1978).
- [2] Pitcher, T., Magurran, A., and Winfield, I., "Fish in larger shoals find food faster," Behavioral Ecology and Sociobiology 10, 149-151 (1982).
- [3] Landeau, L. and Terborgh, J., "Oddity and the 'confusion effect'in predation," *Animal Behaviour* **34**(5), 1372–1380 (1986).
- [4] Larsson, M., "Why do fish school?," Current Zoology 58(1), 116–128 (2012).
- [5] Weihs, D., "Hydromechanics of fish schooling," Nature 241(5387), 290–291 (1973).

- [6] Kalueff, A. V., Gebhardt, M., Stewart, A. M., Cachat, J. M., Brimmer, M., Chawla, J. S., Craddock, C., Kyzar, E. J., Roth, A., Landsman, S., et al., "Towards a comprehensive catalog of zebrafish behavior 1.0 and beyond," Zebrafish 10(1), 70–86 (2013).
- [7] Ashraf, I., Bradshaw, H., Ha, T.-T., Halloy, J., Godoy-Diana, R., and Thiria, B., "Simple phalanx pattern leads to energy saving in cohesive fish schooling," *Proceedings of the National Academy of Sciences* 114(36), 9599–9604 (2017).
- [8] De Bie, J., Manes, C., and Kemp, P. S., "Collective behaviour of fish in the presence and absence of flow," *Animal Behaviour* **167**, 151–159 (2020).
- [9] Saadat, M., Berlinger, F., Sheshmani, A., Nagpal, R., Lauder, G. V., and Haj-Hariri, H., "Hydrodynamic advantages of in-line schooling," *Bioinspiration & Biomimetics* **16**(4), 046002 (2021).
- [10] Liao, J. C., Beal, D. N., Lauder, G. V., and Triantafyllou, M. S., "Fish exploiting vortices decrease muscle activity," Science 302(5650), 1566–1569 (2003).
- [11] Marras, S., Killen, S. S., Lindström, J., McKenzie, D. J., Steffensen, J. F., and Domenici, P., "Fish swimming in schools save energy regardless of their spatial position," *Behavioral ecology and sociobiology* **69**, 219–226 (2015).
- [12] Schreiber, T., "Measuring information transfer," Physical Review Letters 85(2), 461 (2000).
- [13] Bossomaier, T., Barnett, L., Harré, M., and Lizier, J. T., [An introduction to transfer entropy], Springer (2016).
- [14] Boschitsch, B. M., Dewey, P. A., and Smits, A. J., "Propulsive performance of unsteady tandem hydrofoils in an in-line configuration," *Physics of Fluids* **26**(5), 051901 (2014).
- [15] Zhang, P., Rosen, M., Peterson, S. D., and Porfiri, M., "An information-theoretic approach to study fluid–structure interactions," *Journal of Fluid Mechanics* 848, 968–986 (2018).
- [16] Kurt, M., Ormonde, P. C., Mivehchi, A., and Moored, K. W., "Two-dimensionally stable self-organization arises in simple schooling swimmers through hydrodynamic interactions," arXiv preprint arXiv:2102.03571 (2021).
- [17] Giacomello, A. and Porfiri, M., "Energy harvesting from flutter instabilities of heavy flags in water through ionic polymer metal composites," in [Electroactive Polymer Actuators and Devices (EAPAD) 2011], 7976, 90–98, SPIE (2011).
- [18] Giacomello, A. and Porfiri, M., "Underwater energy harvesting from a heavy flag hosting ionic polymer metal composites," *Journal of Applied Physics* **109**(8), 084903 (2011).
- [19] Shannon, C. E., "A mathematical theory of communication," The Bell System Technical Journal 27(3), 379–423 (1948).
- [20] Wiener, N., "The theory of prediction," in [Modern mathematics for engineers: First series], 1, ch. 8, McGraw-Hill (1956).
- [21] Wibral, M., Pampu, N., Priesemann, V., Siebenhühner, F., Seiwert, H., Lindner, M., Lizier, J. T., and Vicente, R., "Measuring information-transfer delays," *PloS one* 8(2), e55809 (2013).
- [22] Sun, J. and Bollt, E. M., "Causation entropy identifies indirect influences, dominance of neighbors and anticipatory couplings," *Physica D: Nonlinear Phenomena* **267**, 49–57 (2014).
- [23] Porfiri, M. and Marín, M. R., "Symbolic dynamics of animal interaction," *Journal of theoretical biology* **435**, 145–156 (2017).